




# Characterization and thermal stability study of efavirenz and solid dispersion with PVPVA 64 by means of thermal analysis and pyrolysis coupled with GC/MS

Salvana Priscylla Manso Costa<sup>1</sup> · Tarcyla de Andrade Gomes<sup>2</sup> · Keyla Emanuelle Ramos da Silva<sup>3</sup> · Paulo Cezar Dantas da Silva<sup>2</sup> · Adriana Eun He Koo Yun<sup>2</sup> · Taynara Batista Lins Melo<sup>4</sup> · Fabrício Havy Dantas de Andrade<sup>4</sup> · Fabio Souza Santos<sup>4</sup> · Rosali Maria Ferreira da Silva<sup>2</sup> · Larissa Araújo Rolim<sup>5</sup> · Pedro José Rolim Neto<sup>2</sup> 

Received: 27 February 2019 / Accepted: 6 October 2020 / Published online: 29 October 2020  
© Akadémiai Kiadó, Budapest, Hungary 2020

## Abstract

The acquired immunodeficiency syndrome remains a major problem in worldwide public health and its antiretroviral treatment therapy combines at least three high activity classes of drugs. Access to antiretroviral treatment for HIV-infected patients is a global public health priority and efavirenz (EFZ) is one of the first drug choices. However, EFZ is classified as a class II drug, according to the biopharmaceutics classification system due to low solubility and high permeability, which leads it to fail in absorption and hence bioavailability. One of the approaches used to overcome these issues is the preparation of solid dispersions. In this study, thermal analysis and pyrolysis coupled with gas chromatography-mass spectrometry (GC/MS) were employed to determine efavirenz thermal stability and the solid dispersion with poly (vinylpyrrolidone-co-vinylacetate) (PVPVA 64). Thus, it suggests that EFZ was converted to its amorphous state, and there was an increase in EFZ thermal stability when it is dispersed in a polymer matrix compared to the drug alone, since there was an increase in the activation Energy ( $E_a$ ) and a decrease in frequency factor ( $A$ ). Furthermore, there was a change in the zero reaction order to one. The thermal stability time of the formulation was estimated at 7 months. In addition, it was possible to observe a good correlation between loss of mass and the technique of Pyrolysis-GC-MS and to posit the formation of new fragments, which clarifies the technique with regard to the identification of thermal decomposition fragments.

**Keywords** Efavirenz · Solid dispersion · PVPVA 64 · Thermal analysis DSC-photovisual · Pyrolysis-GC-MS

## Introduction

Efavirenz (EFZ) is considered one of the most used anti-HIV drugs, however, like the vast majority of antiretrovirals, it is classified as a class II drug, according to the biopharmaceutics classification system (BCS), for exhibiting low

solubility and high permeability [1, 2]. It is known that the aqueous solubility of a drug is a prerequisite to absorption and, therefore, it is one of the major barriers to the effectiveness of the drug. Thus, the increase, by means of pharmaceutical technology, of the aqueous dissolution and, consequently, the bioavailability of poorly soluble drugs in

✉ Pedro José Rolim Neto  
rolim.pedro@gmail.com

<sup>1</sup> Laboratory of Nanotechnology and Nanomedicine - Institute of Technology and Research, Universidade Tiradentes, Murilo Dantas Avenue, 300, Farolândia, Aracaju, SE 49.032-490, Brazil

<sup>2</sup> Laboratory of Medicine Technology - Department of Pharmaceutical Sciences, Federal University of Pernambuco, Professor Arthur de Sá Street, s/n, Cidade Universitária, Recife, PE 50740-521, Brazil

<sup>3</sup> Institute of Exact Sciences and Technology, Federal University of Amazonas, Nossa Senhora do Rosário Street, 3863, Tiradentes, Itacoatiara, AM, Brazil

<sup>4</sup> Unified Drug Development and Testing Laboratories - Department of Pharmaceutical Sciences, Federal University of Paraíba, Campus I, João Pessoa, PB 58059-900, Brazil

<sup>5</sup> Analytical Center – College of Pharmaceutical Sciences, Federal University of Vale do São Francisco, José de Sá Maniçoba Avenue, s/n, Centro, Petrolina, PE 56304-917, Brazil

water is considered as one of the most challenging aspects in modern drug development [3]. Solid dispersion (SD) is considered a major technique for increasing solubility and it aims, by means of molecular processes, to change the crystalline form of the drug into its amorphous state [3–5].

Solid dispersions exhibit complex physicochemical properties, so due to this, there is a need for the use of analytical methods that will allow for its full characterization. For pharmaceutical purposes, the use of thermal analysis is described in the characterization, in the determination of purity and moisture, in polymorph identification, in the evaluation of the stability of drugs and in medicines by means of thermal degradation kinetic studies [6]. Another great potential is its use in the characterization of SD, which according to Baird and Taylor [7], one of the main contributions of this technique is the determination of the physical stability of SD, primarily, through the evaluation of molecular mobility, crystallization behavior and miscibility between the drug and polymer.

Thermal decomposition kinetics is considered an essential element in thermal analysis since, starting from the results obtained, the decomposition reaction mechanism, as well as, the parameters of the Arrhenius equation can be determined (activation energy, frequency factor and reaction order). [8] Interestingly, thermoanalytical study cannot replace the classic stability studies, but, from it, data are extracted that provide valuable information on storage conditions, especially, useful life, half-life and shelf life, which are considered of paramount importance in the development of new pharmaceuticals [9, 10].

Thus, the objective of this work was to study the thermal stability of EFZ and SD with PVPVA-64 by means of thermal analysis (isothermal and dynamic methods) and pyrolysis coupled with GC/MS.

## Materials and methods

### Raw materials and solvents

Efavirenz (Cristália<sup>®</sup>, Lot: 1289/07) (S)-(–)-6-chloro-4-(cyclopropylethynyl)-4-(trifluoromethyl)-2,4-dihydro-1*H*-3,1-benzoxazin-2-ona, donated by LAFEPE<sup>®</sup>, with an estimated purity, by means of the high efficiency liquid chromatography technique, of 98%. The polymers used were: PVP-K30, Soluplus<sup>®</sup>, PVPVA-64, the last two donated by the University of Toronto. Methyl alcohol, acetonitrile, absolute ethanol and ultra-purified water were also used.

### Obtaining solid dispersions (SD)

The amounts of EFZ (10%) and the polymer, PVPVA 64, were carefully weighed, in suitable proportions, and were

separately dissolved in acetonitrile and methanol to solubilize the EFZ and to solubilize the PVPVA 64. The solutions were mixed and, subsequently, maintained for 15 min in ultrasound. The solvent was completely removed by evaporation at  $60 \pm 5$  °C under normal pressure in an oven. The thin layer obtained with each SD was pulverized and sieved in a 425 micron mesh. The thin layer obtained was pulverized with the aid of a porcelain mortar, pestle and a small amount of liquid nitrogen to facilitate the spraying process in addition to avoiding the induction of drug crystallization due to heat. The resulting SD was sieved in a 425 micron mesh, packed in hermetically sealed vials and stored in a vacuum desiccator with controlled humidity.

### Thermal analysis

#### Differential scanning calorimetry (DSC)

The DSC curves of the isolated compounds and the SD system that showed the best performance in the dissolution study in vitro were obtained in a Setaram LABSYS evo<sup>®</sup>-TG-DSC 1600 °C scanning calorimeter connected to Calisto Acquisition software with an argon atmosphere and heating rate of 10 °C min<sup>-1</sup> at a 25–500 °C temperature range. An aluminum sample holder and a sample mass equivalent to  $10 \pm 0.2$  mg were used. Determinations were performed in triplicate. Indium and zinc were used to calibrate the temperature range and enthalpy response.

#### Thermogravimetry (TG)

The thermoanalytical characterization by TG of the isolated compounds and the SD system that showed the best performance in the dissolution study in vitro was performed in triplicate by means of a Shimadzu<sup>®</sup> TGA model Q60 thermobalance in a nitrogen atmosphere with a flow of 50 mL min<sup>-1</sup>. The sample mass was about  $1 \pm 0.5$  mg of EFZ, placed in an aluminum crucible at a 25–600 °C temperature range and a heating rate of 10 °C min<sup>-1</sup>. Before starting the experiment, the equipment was checked that it was running normally by performing a previous test of standard calcium oxalate monohydrate according to the ASTM E1582-93 (The American Society for Testing and Materials, 1993) [11–13].

#### DSC-photovisual

DSC studies of the isolated compounds and the SD system that showed the best performance in the dissolution study in vitro were performed in a Shimadzu<sup>®</sup> DSC-50 calorimeter in a nitrogen atmosphere at a flow rate of 50.0 mL min<sup>-1</sup> and a heating rate of 10 °C min<sup>-1</sup> up to 500 °C. The DSC was linked to a system involving an Olympus<sup>®</sup> microscope

connected to a Sanyo<sup>®</sup> VCC-D520 camera with a high resolution image. Samples (2 mg) were placed in an aluminum sample holder, and then, it was sealed hermetically. The temperature and the heat flux of the DSC instrument were calibrated by the melting point and the enthalpy of standard indium and zinc [14, 15].

### Thermal degradation kinetics

The determination of the kinetic parameters through TG can be performed by isothermal and dynamic methods. The kinetic investigation of non-isothermal degradation of the SD system that showed the best performance in the dissolution study in vitro was obtained from TG data by applying the Ozawa method. For the experiment to be performed, samples (~ 10 mg) were placed in aluminum pans and heated to a temperature range of 30–600 °C at heating rates equal to 7.5, 10 and 15 °C min<sup>-1</sup> under a dynamic nitrogen atmosphere (N<sub>2</sub>) with a flow rate of 50 mL min<sup>-1</sup> [9, 16].

For the kinetic isothermal study, TG curves were obtained by heating the samples up to temperatures of 245, 250, 255, 260 and 265 °C and maintained at isothermal conditions in a N<sub>2</sub> atmosphere (50 mL min<sup>-1</sup>) during the necessary time for a 5% ± 0.5 loss of mass in the aluminum sample port with approximately a 4 mg sample.

The heating procedure was performed as described in Table 1, in order to reach the working temperature in less time. Thus, the sample was heated to 200 °C at a rate of 20 °C min<sup>-1</sup>; subsequently, it was heated at a rate of 10 °C min<sup>-1</sup> to 20 °C below the desired isotherm (*T*<sub>iso</sub>) temperature. Upon achieving this working isothermal temperature, it remained for 170 min.

### Theoretical approach

Thermogravimetric analysis (TGA) is one of the most commonly used techniques to study the reactions of decomposition of solids.

Thermokinetic data corresponding to the decomposition reaction could be calculated for determination of some parameters such triplet kinetic on thermal behavior

**Table 1** Heating program to obtain the isothermal thermogravimetric curves

Heating rate/°C min <sup>-1</sup>	Temperature/°C	Time/min
20	200	—
10	Isothermal temperature—20 °C	—
2	Isothermal temperature	170

of drugs and medicine compounds. Estimation of kinetic triplet of drugs is in solid state that are useful in obtaining knowledge about drug decomposition reactions.

The conversion fraction ( $\alpha$ ) was defined by the expression:

$$\alpha = \frac{m_0 - m_t}{m_0 - m_f} \times 100 \quad (1)$$

where  $m_0$  is the initial mass of sample,  $m_t$  is the mass of the sample at time  $t$ , and  $m_f$  is the final mass of the sample in the process.

In kinetic analysis, the equation of the process can be written as follows [17]:

$$d\alpha/dt = k \cdot f(\alpha) \quad (2)$$

where  $\alpha$  is the conversion fraction,  $k$  is rate constant for the process described by the Arrhenius equation (Eq. 3),  $f(\alpha)$  is the conversion function for a solid-state reaction depends on the reaction mechanism [17].

$$k = A \exp - \frac{E_a}{RT} \quad (3)$$

where  $A$  is the pre-exponential factor,  $E$  is the apparent activation energy,  $T$  is the absolute temperature, and  $R$  is the gas constant. If the constant heating rate  $\beta$  is applied, yields combination of Eqs. (2) and (3) to the relationship:

$$\frac{d\alpha}{dT} \beta = A \left( \exp - \frac{E}{RT} \right) f(\alpha) \quad (4)$$

Several authors suggested different ways based on kinetic study performed under non-isothermal conditions. The kinetic parameters may be determined from TG curves by using the isoconversional methods: Friedman, Kissinger–Akahira–Sunose e Flynn–Wall–Ozawa which involves measuring the temperatures corresponding to fixed values of  $\alpha$  from experiments at different heating rates [18].

### Kissinger–Akahira–Sunose method (KAS)

The KAS method is a integral method sometimes called the generalized Kissinger method is one of the best isoconversional methods, and it is based on the equation:

$$\ln \frac{\beta}{T^2} = \ln \frac{AR}{Eg(x)} - \frac{E}{RT} \quad (5)$$

The Kissinger method is based on the calculation of activation energy from a point of the maximal temperature,  $T$ , and the activation energy can be determined from the slope of the line obtained by plotting  $\ln(\beta/T^2)$  versus  $1/T$ .

### Friedman method (FD)

The isoconversional Friedman method is based on the equation:

$$\ln\left(\frac{dx}{dt}\right) = \ln\left(\beta \frac{dx}{dT}\right) = \ln[Af(x)] - \frac{E}{RT} \quad (6)$$

In order to calculate the activation energy more precisely, the term  $\ln(d\alpha/dT)$  was obtained by numerical derivation of the curve  $\alpha$  versus  $T$  with respect to  $T$  and subsequent taking logarithms. The plot  $\ln[\beta(d\alpha/dT)]$  versus  $(1/T)$  was used to obtain from the slopes of the straight lines and determine the activation energy

### Flynn–Wall–Ozawa method (FWO)

The isoconversional method proposed by Flynn–Wall–Ozawa using Doyle's approximation. This method can be used for determination of the  $E_a$  values without any knowledge of the reaction mechanisms and is based on the equation:

$$\log \beta = \log \frac{AE_a}{Rg(\alpha)} - 2.315 - 0.4567 \frac{E_a}{RT} \quad (7)$$

From the slopes of the straight lines obtained by the graphic plot  $\log \beta$  versus  $(1/T)$  was determined the activation energy.

### Reaction mechanism in a solid reaction process

The kinetic model of process can be determined using the Criado method. Using as reference point  $\alpha = 0.5$ , the following equation are easily derived from Eqs. (2) and (4):

$$\frac{Z(x)}{Z(0.5)} = \frac{f(x)g(x)}{f(0.5)g(0.5)} = \left(\frac{T_x}{T_{0.5}}\right)^2 \frac{\left(\frac{dx}{dt}\right)_x}{\left(\frac{dx}{dt}\right)_{0.5}} \quad (8)$$

Equation (8) is used to represent the experimental curve based in different models listed in Table 2. Thus, by comparing these two curves, the type of mechanism involved in the thermal degradation can be identified.

### Pyrolysis-GC/MS

The pyrolysis studies were conducted in the pyrolyzer attached to a gas chromatograph (Shimadzu® GC/MS—QP5050A) directly connected to a mass spectrometer using electrons as a source of ionization. The EFZ solid-state sample was placed in a platinum crucible and introduced into the pyrolyzer for each experimental group, which showed isothermal temperatures equal to 270, 400 and 500 °C.

Fragmentation was performed by electron impact with an ionization energy of 70 eV. The spectrometer was operated in scan mode, scanning in the range of 50–600  $m/z$ . The temperature of the ion source was

**Table 2** Kinetic model functions  $f(\alpha)$  and corresponding  $g(\alpha)$  usually employed for the solid-state reactions

Reaction model	Differential form	Integral form
<i>Nucleation models</i>		
Power law ( $P_2$ )	$2\alpha^{1/2}$	$\alpha^{1/2}$
Power law ( $P_3$ )	$3\alpha^{2/3}$	$\alpha^{1/3}$
Power law ( $P_4$ )	$4\alpha^{3/4}$	$\alpha^{1/4}$
Nucleation and growth Avrami–Erofev ( $A_2$ )	$2(1-\alpha)[- \ln(1-\alpha)]^{1/2}$	$[- \ln(1-\alpha)]^{1/2}$
Nucleation and growth Avrami–Erofev ( $A_3$ )	$3(1-\alpha)[- \ln(1-\alpha)]^{2/3}$	$[- \ln(1-\alpha)]^{2/3}$
Nucleation and growth Avrami–Erofev ( $A_4$ )	$4(1-\alpha)[- \ln(1-\alpha)]^{3/4}$	$[- \ln(1-\alpha)]^{3/4}$
<i>Geometrical contraction models</i>		
Phase boundary controlled reaction (one-dimensional movement) ( $R_1$ )	1	A
Phase boundary controlled reaction (contracting area) ( $R_2$ )	$2(1-\alpha)^{1/2}$	$1 - (1-\alpha)^{1/2}$
Phase boundary controlled reaction (contracting volume) ( $R_3$ )	$3(1-\alpha)^{2/3}$	$1 - (1-\alpha)^{1/3}$
<i>Diffusion models</i>		
One-dimensional diffusion ( $D_1$ )	$1/(2\alpha)$	$\alpha^2$
Three-dimensional diffusion (equação de Jander) ( $D_3$ )	$-[1/\ln(1-\alpha)]$	$((1-\alpha)\ln(1-\alpha)) + \alpha$
Three-dimensional diffusion (equação de Ginstling-Brounshtein) ( $D_4$ )	$3/[2((1-\alpha) - 1/3 - 1)]$	$1 - (2/3)\alpha - (1-\alpha)^{2/3}$
<i>Reaction order models</i>		
Zero order (F0/R1)	1	A
Mampel (first order) (F1)	$(1-\alpha)$	$-\ln(1-\alpha)$
Second order (F2)	$(1-\alpha)^2$	$[1/(1-\alpha)] - 1$
Third order (F3)	$(1-\alpha)^3$	$(1/2)[(1-\alpha)^{-2} - 1]$

300 °C. The separation of the fragments was carried out using a capillary column with a phenyl stationary phase: dimethylpolysiloxane (5:95) with 30 m length, 0.25 mm internal diameter and 0.25 mm particle size. The column temperature was set to a heating rate of 15 °C min<sup>-1</sup> to a final temperature of 280 °C. Helium gas was used as gas stripping at a flow rate of 1.0 mL min<sup>-1</sup>. The identification of compounds was performed by comparing the mass spectra obtained with the Wiley/NBS library<sup>®</sup> [19–21].

## Results and discussion

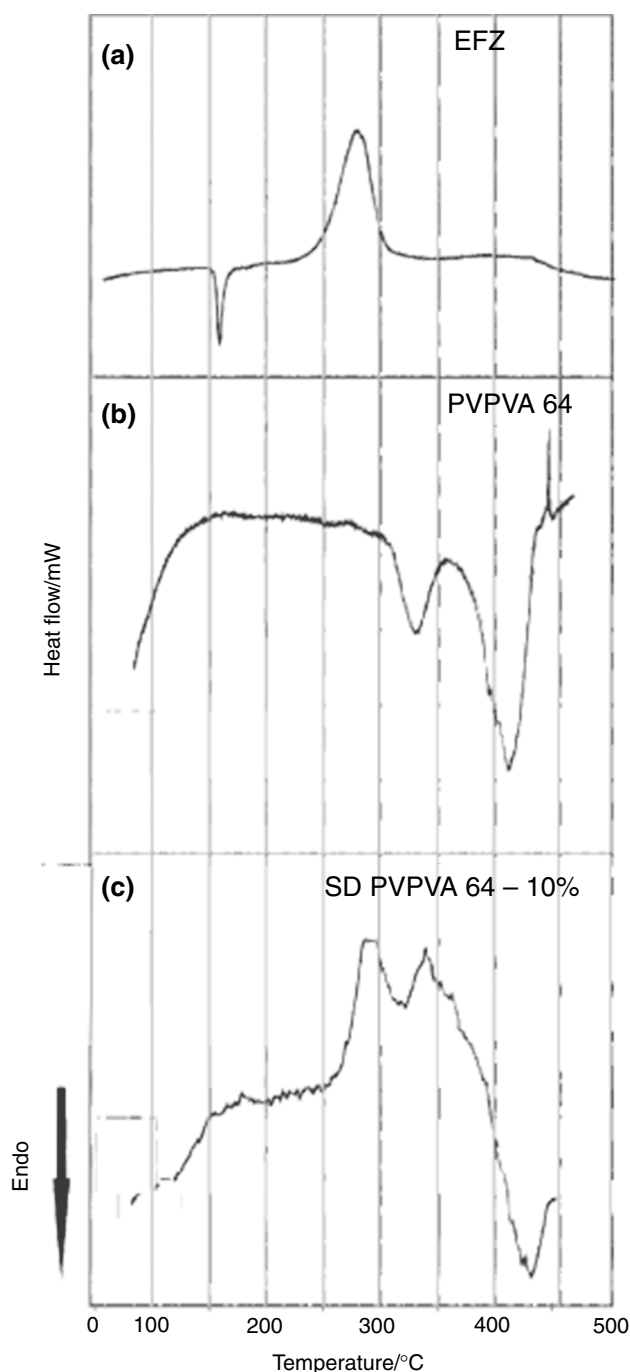
### Thermal characterization

Figures 1 and 2 show DSC and TG curves for EFZ, PVPVA 64 and SD 64 PVPVA EFZ, 10%, respectively. The DSC curve for EFZ showed an endothermic peak corresponding to the fusion event ( $T_{\text{peak}} = 140$  °C;  $T_{\text{onset}} = 138$  °C;  $\Delta H_{\text{fusion}} = -70.58$  J g<sup>-1</sup>), characterizing the drug in its crystalline form. The exothermic events in the sequence correspond to the degradation process that occurs in a single defined stage as shown in the TG curve (Fig. 1a), in the temperature range of 200 °C to 300 °C and with a loss of mass of  $\Delta m = 86.16\%$  [10, 16].

In Fig. 1b PVPVA 64 Tg can be observed in the range of 100–104 °C represented by a slight change in the baseline, followed by two endothermic events related to its degradation which can best be seen in the TG curve (Fig. 2b). This process occurs in two well-defined events. The first event, in the temperature range between 270 and 350 °C and the second, between 350 and 450 °C, proved to be a very stable thermoplastic polymer [22].

For pharmaceutical purposes, the use of thermal analysis is described in the characterization, determination of purity and moisture, polymorph identification, evaluation of the stability of drugs and medicines through thermal degradation kinetic studies [6]. Another great potential is its use in the characterization of SD, which, according to Baird and Taylor [7], one of the main contributions of this technique is the determination of the physical stability of a SD, primarily, through the evaluation of molecular mobility, crystallization behavior and miscibility between the drug and polymer.

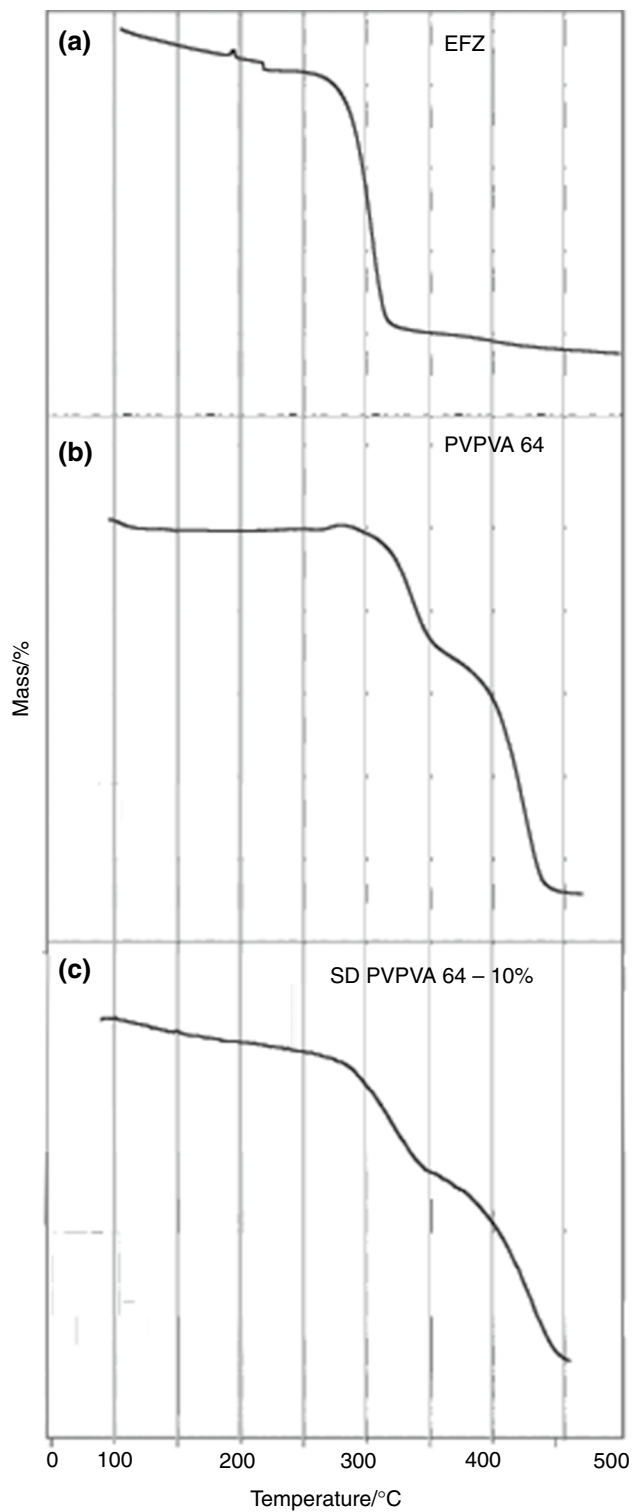
Analyzing the DSC curve (Fig. 1c), it was observed that the drug melting peak disappeared, suggesting that EFZ was converted into its amorphous state. In addition, the TG (Fig. 2c) curve showed that the SD remained thermally stable up to a temperature of 270 °C, suggesting that the polymer provided thermal protection for the drug.



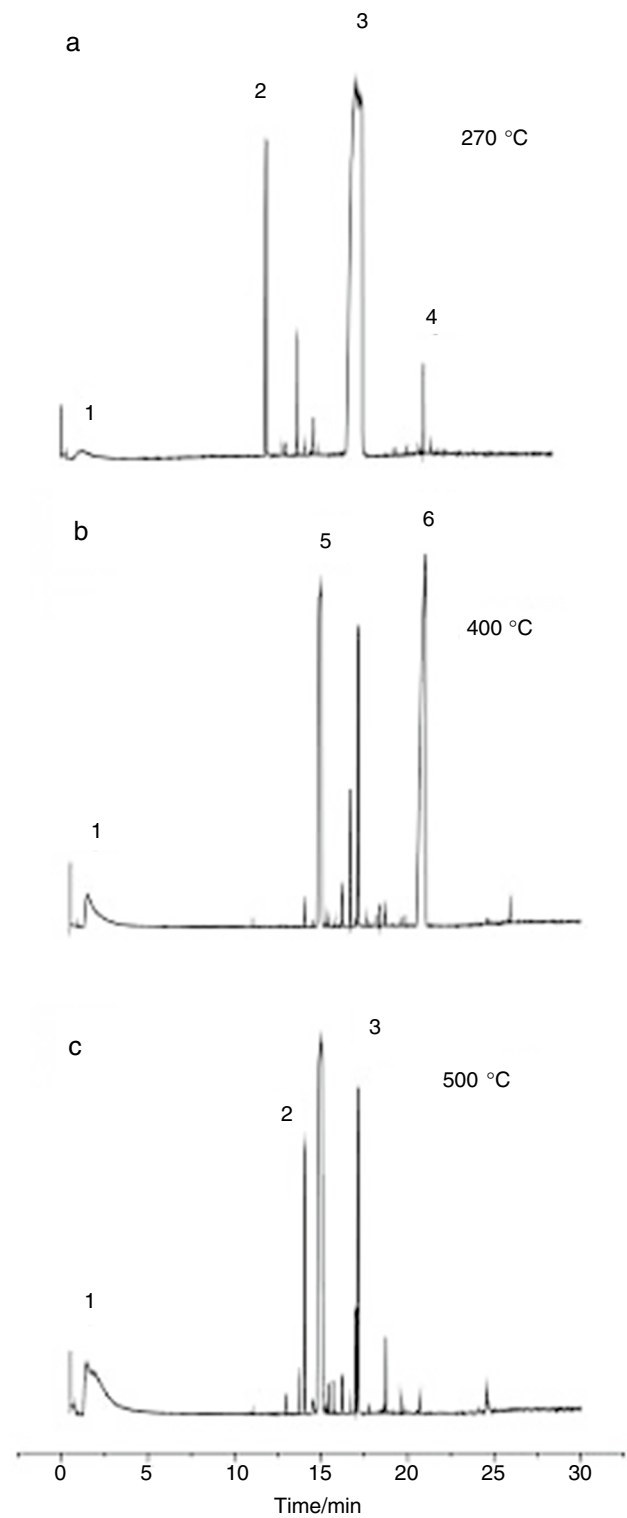
**Fig. 1** DSC curves for EFZ (a), PVPVA 64 (b) and SD PVPVA 64—EFZ 10% (c) obtained in a dynamic atmosphere of nitrogen (50 mL min<sup>-1</sup>) and a heating rate of 10 °C min<sup>-1</sup>

### Pyrolysis-GC/MS

The degradation products corresponding to the EFZ loss of mass phase were identified by pyrolysis coupled with GC/MS. Figure 3 shows the pyrograms obtained at temperatures of 270, 400 and 500 °C, where it was



**Fig. 2** TG curves for EFZ (a), PVPVA 64 (b) and SD PVP VA 64—EFZ 10% (c) obtained in an atmosphere of dynamic nitrogen ( $50 \text{ mL min}^{-1}$ ) and a heating rate of  $10 \text{ }^\circ\text{C min}^{-1}$

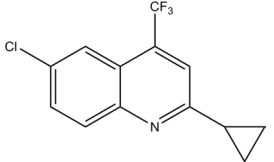
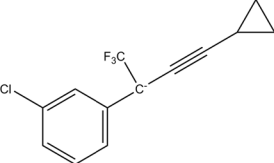
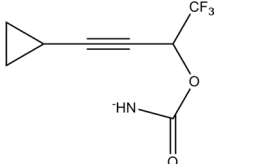
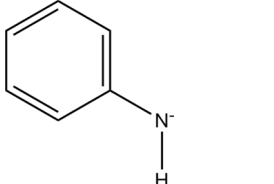
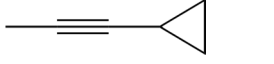


**Fig. 3** Pyrograms obtained from EFZ at temperatures of 270, 400 and 500 °C showing the degradation products of the thermal decomposition process of the drug

possible to identify the fragmented EFZ during thermal decomposition.

The peak of the EFZ molecular ion was not identified in the mass spectra (MS). It was confirmed, thereby, that in the temperature range of 230 to 255 °C loss of mass observed in

**Table 3** EFZ thermal degradation products obtained by GC/MS pyrolysis

Peak	<i>m/z</i>	Molecular formula	Structural formula
1	44	CO <sub>2</sub>	<chem>O=C=O</chem>
2	270	C <sub>13</sub> H <sub>9</sub> ClN F <sub>3</sub>	
3	256	C <sub>13</sub> H <sub>8</sub> ClNOF <sub>3</sub>	
4	207	C <sub>8</sub> H <sub>7</sub> O <sub>2</sub> NF <sub>3</sub>	
5	91	C <sub>6</sub> H <sub>6</sub> N	
6	77	C <sub>6</sub> H <sub>5</sub>	

the TGA curve (Fig. 2a) corresponds to the degradation of the drug. This fact means that, beginning at this temperature, there is no presence of intact EFZ [19, 20].

Through knowledge of the EFZ degradation mechanism by hydrolysis as proposed by Maurin et al. [23] it was possible to identify the same degradation products obtained in the thermal decomposition by pyrolysis, such as were proposed for other products, which are summarized in Table 3.

Thus, it suggests, possibly, that EFZ undergoes thermal fragmentation at its sites that are more susceptible to breakage since the majority of observed fragments appeared at different temperatures which showed that, perhaps, they do not undergo secondary fragmentation, which makes the technique in the identification of thermal decomposition fragments clear.

### DSC-photovisual

The DSC-photovisual shows a microscope attached at the top of the equipment, permitting visualization of morphological changes of the sample during heating and/or cooling [12].

Images captured during the analysis of the EFZ DSC-photovisual, the PVPVA 64 and SD PVPVA 64—EFZ 10% are illustrated in Figs. 4–6, respectively.

In Fig. 4d, the EFZ fusion event followed by its decomposition (Fig. 4i–l) can be observed, whereas in Fig. 5b the beginning of the vitreous transition process of the polymer with subsequent degradation can be seen (Fig. 5i–l). Figure 6 shows the absence of the crystalline form of EFZ in the SD results, also corroborated by DSC analysis, subsection 3.1, since the curve showed no melting peak related to the drug.

The vitreous transition event is typical for amorphous solids, such as polymers under study, since they have the ability to exhibit the behavior of both a fluid and a solid depending on the system temperature. Thus, at low temperatures,

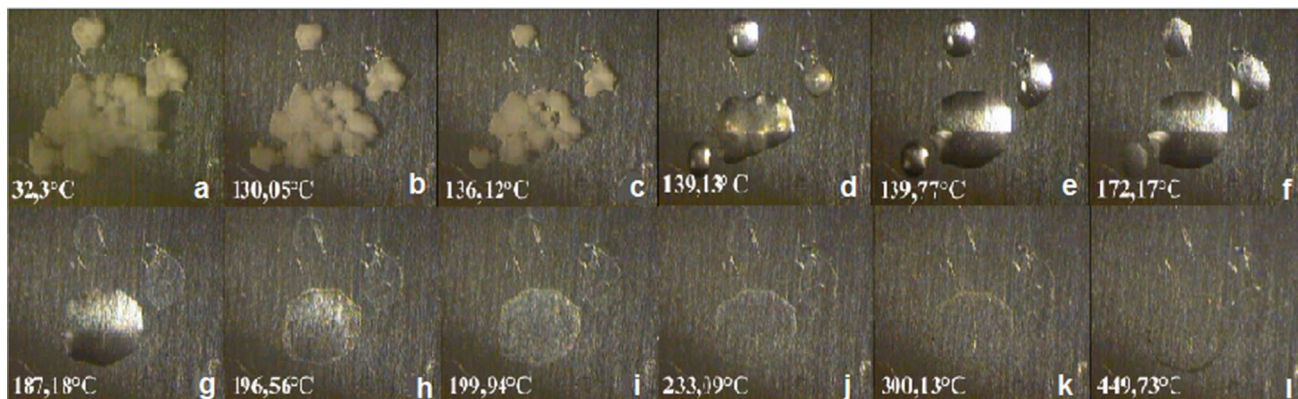


**Fig. 4** Photomicrographs of the DSC-photovisual of EFZ

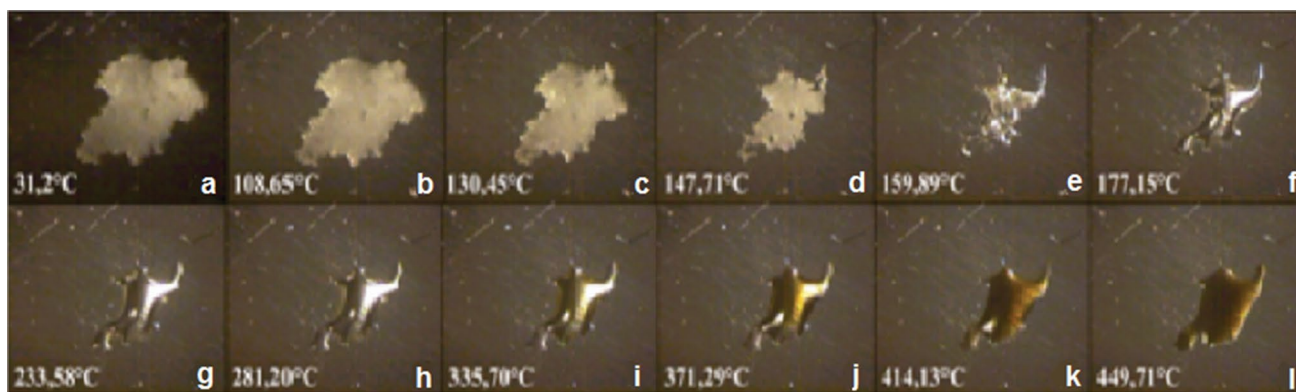


Fig. 5 Photomicrographs of the DSC-photovisual of PVPVA 64

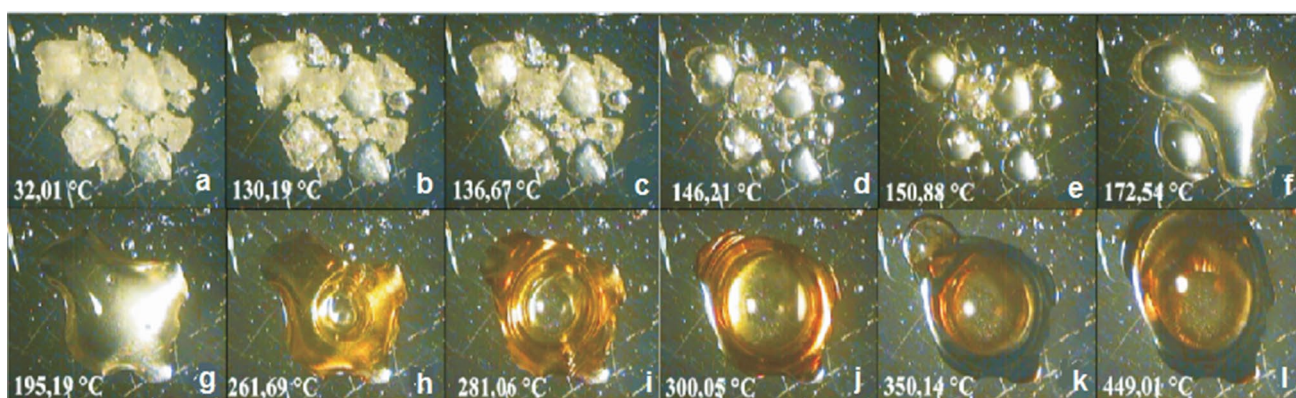


Fig. 6 Photomicrographs of the DSC-photovisual of SD PVPVA 64—EFZ 10%

amorphous materials exhibit structural properties of normal solids, but at a certain temperature known as the vitreous transition temperature ( $T_g$ ) these materials begin to exhibit a viscous state. [7, 24].

Thus, in Fig. 6d–g you can visualize the transition from solid to viscous PVPVA 64, but at a temperature higher than the isolated polymer, thus, favoring the reduction of molecular mobility of the system and, consequently, the increase of the stability of the amorphous form of the drug. Then, the change from yellow to dark brown color could be observed, suggesting the deterioration of the SD according to the TG curve (Fig. 2) [14, 15, 25, 26].

### Degradation kinetics

In this study, the Ozawa method was used, available in the TASYs Shimadzu software (Kinetic Analysis TGA), and performed using non-isothermal TG curves. The method is based on integral calculation starting with the Arrhenius equation to calculate the kinetic parameters in the early stage of thermal decomposition at around 270–340 °C. This step represents the first loss of mass event, which is theoretically

associated with the degradation of EFZ in SD. To apply this method it is necessary to obtain, at least, three TG curves in different ratios of heating. This study used three TG curves at heating rates of 7.5, 10 and 15 °C min<sup>-1</sup>.

In Fig. 7, the SD TG curves are shown, which were obtained by the non-isothermal method together with the heating rate logarithm chart in lieu of the inverse of the absolute temperature, after processing data by the Ozawa method, while in Fig. 8, the residual mass  $G(x)$  chart can be observed in lieu of reduced time. Beginning with the plotting of the chart  $G(x)$ , in lieu of the reduced time (min), which promotes the formation of a straight line, one can choose the best reaction mechanism by means of statistical processing of the linear regression model, making the choice of the linear correlation coefficient value ( $r^2$ ) that which is nearest to the unit (Table 4).

In this case, the first degradation event was characterized as a first-order reaction ( $n = 1$ ) for presenting  $r^2 = 0.9861$ , which is considered more significant than that obtained for  $n = 0$  and  $n = 2$ . The other kinetic parameters were measured from the choice of the best reaction model. The  $aE$ , calculated by the Ozawa method, showed a value



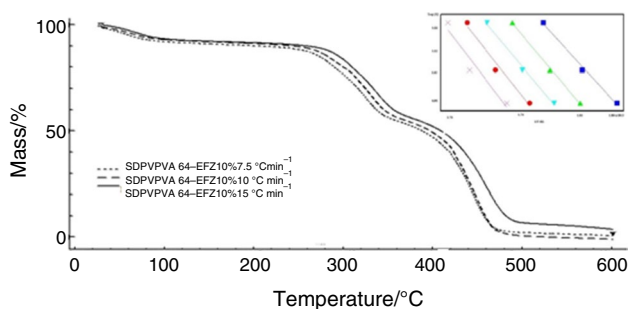


**Fig. 7** TG curves and the Ozawa chart of SD PVP VA64—EFZ 10% obtained in five ratios of heating under a dynamic nitrogen atmosphere using the non-isothermal method

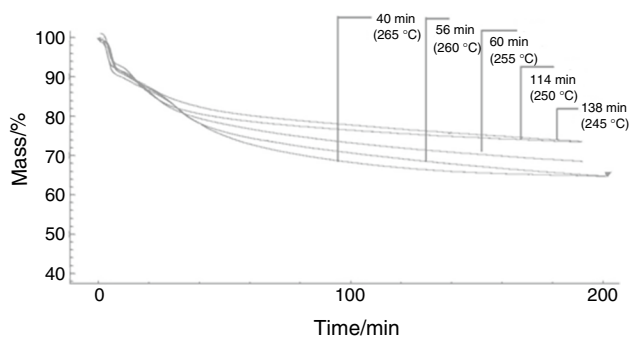


**Fig. 9** DS EFZ/KL 10% isotherm curves at different temperatures in an atmosphere of N<sub>2</sub> (50 mL min<sup>-1</sup>)

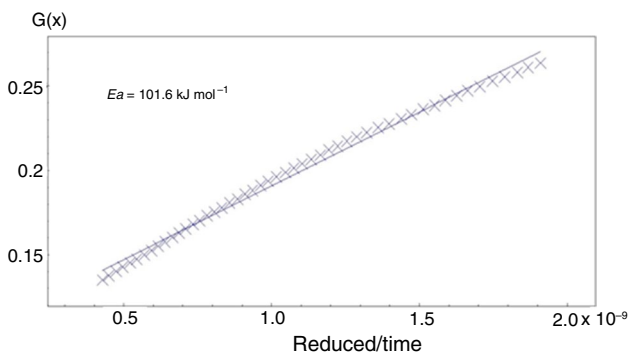


**Fig. 8** Residual mass  $G(x)$  as a function of reduced time

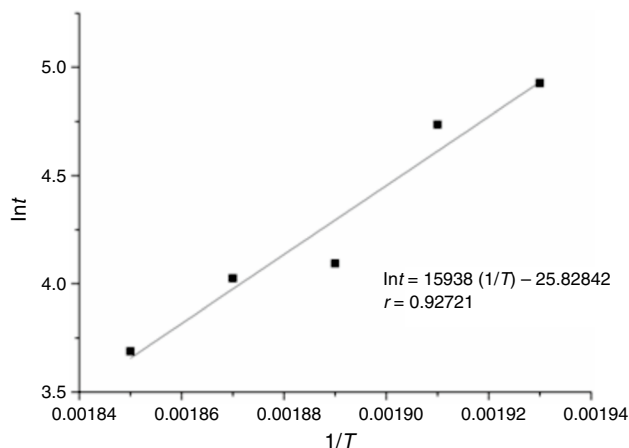


**Fig. 10** Arrhenius plot

**Table 4**  $r^2$  from the order of kinetic reactions of degradation obtained by the non-isothermal model

$r^2$	$r^2$	$r^2$
Zero order reaction	One order reaction	Two order reaction
0.9827	0.9861	0.7995

of 101.6 kJ mol<sup>-1</sup> and A 8, 724 × 10<sup>7</sup> min<sup>-1</sup> (Table 4). These parameters were different when compared to the drug alone. [10, 16].

There was an increase and a decrease in A resulting, thereby, in increased EFZ stability, as well as, the order of reaction which changed from zero to one. The result suggests that the degradation reaction involves more than one SD step which occurs through complex mechanisms [27].

The superposition of three TG curves, obtained at different heating rates, are shifted to higher temperatures when heating rates increase. A linear trend is shown in the correlation of the three curves represented by the Ozawa chart [9, 10, 27].

The isothermal TG curves for the first stage of decomposition of the SD-EFZ/KL 10% are shown in Fig. 9. These curves show the dependence of the rate of loss of mass in the isotherm with the temperature, i.e., the higher the temperature the less time required to achieve the same loss of mass. These curves were used to plot the ln t chart versus the inverse of the temperature, 1/T (K<sup>-1</sup>), also called the Arrhenius plot, where the straight line equation was obtained by linear regression ( $y = ax + b$ ) to evaluate the validity of the kinetic model, to measure the linearity and  $r^2$  (Fig. 10) [9, 10].

Furthermore, these curves were used to perform the calculations for determining the order of reaction using the Arrhenius model. These data were plotted and are shown in Table 5. The choice of the reaction order was determined starting from the values of  $r^2$ , whose values that were closer to the unit was the sorting order, confirming the order one.

The value of aE for SD PVPVA 64—EFZ 10% was 132.508 kJ mol<sup>-1</sup>, calculated beginning with the product of the angular coefficient slope with the general constant of the gases (R) (8.314 J mol<sup>-1</sup> K<sup>-1</sup>) (Table 6).

**Table 5** Correlation of the kinetic reaction orders of isothermal degradation at temperatures of 245, 250, 255, 260 and 265 °C SD PVP VA64—EFZ 10%

Temperature/°C	$r^2$	$r^2$	$r^2$
	Zero order reaction	One order reaction	Two order reaction
245	0.9893	0.994	0.9919
250	0.9657	0.9739	0.97
255	0.9153	0.9831	0.978
260	0.9847	0.9922	0.9888
265	0.8806	0.9008	0.8909
Mean	0.94712	0.96688	0.96392

**Table 6** Activation energy and kinetic parameters obtained by non-isothermal and isothermal methods

Sample	Non-isothermal				Isothermal		
	$E_a/kJ\ mol^{-1}$	$A/min^{-1}$	Order of reaction	$r^2$	$E_a/kJ\ mol^{-1}$	Order of reaction	$r^2$
EFZ*	93.24	$1.67 \times 10^8$	0	–	91.58	0	0.9634
SD PVP VA 64/EFZ 10%	101.6	$8.72 \times 10^7$	1	0.9861	132.508	1	0.9669

The stability (in days), based on the Arrhenius equation, using 25 °C as a standard temperature, was calculated. The result was an estimated time of thermal stability of 214 days, or about 7 months for a decay of 10% by mass.

An increase of SD aE can be observed, irrespective of the method used, when compared with the isolated EFZ; this result may suggest an absence of incompatibility between the polymer and the drug, as well as an increase in thermal stability.

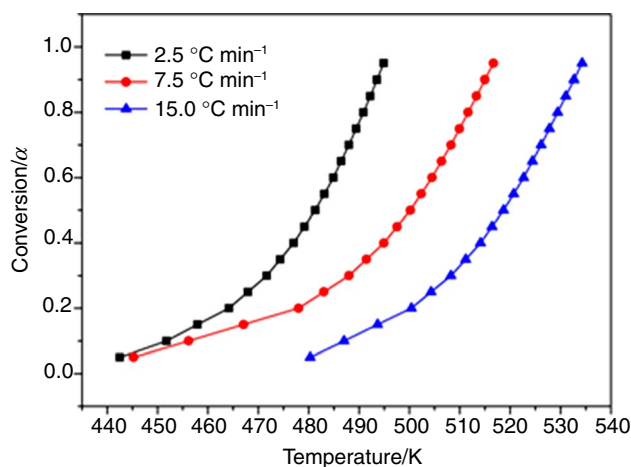
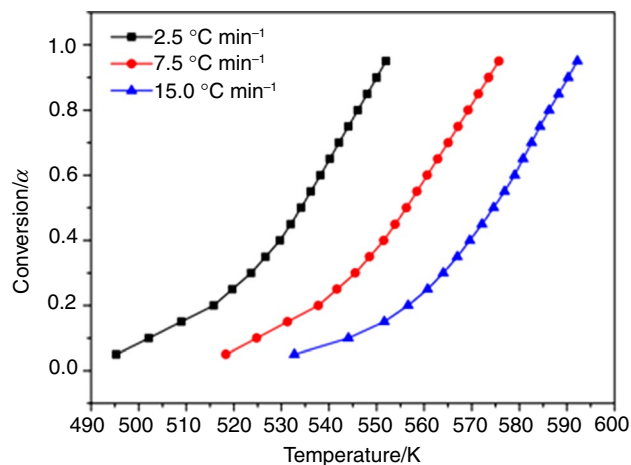
Combined experiments, using isothermal and non-isothermal conditions, are considered the best way to correctly determine kinetic parameters [27]. In this case, it was possible to perceive that good application of the methods used, in view of the value of  $r^2$ , in the linear correlation, was close to one.

## Kinetic results

As it has been mentioned above, the kinetic study of drugs and medicines by isothermal and non-isothermal methods are very important to determine the kinetic parameters such as activation energy, frequency factor and reaction order [20].

In order to proceed with the kinetic analysis of the experimental data of EFZ and SD-EFZ-PVPVA64, the following methods were used: KAS, FD and FWO method. As seen in Figs. 11 and 12 the relation between conversion degree and temperature depends on the heating rate.

In the Fig. 13, the plots shown a straight line obtained through linear fit, whose slope gives  $-E_a/R$  value from which is obtained the activation energy for both samples. Comparing the results of the kinetic parameters from both methods it can be verified differences between values found. The linearization plots for these methods are shown in Fig. 14. The linearization plots for both integral models is marked by a parallelism among the linear regressions obtained at each

**Fig. 11** Curves of conversion degree versus temperature of EFZ**Fig. 12** Curves of conversion degree versus temperature of EFZ-SD-PVPVA-64

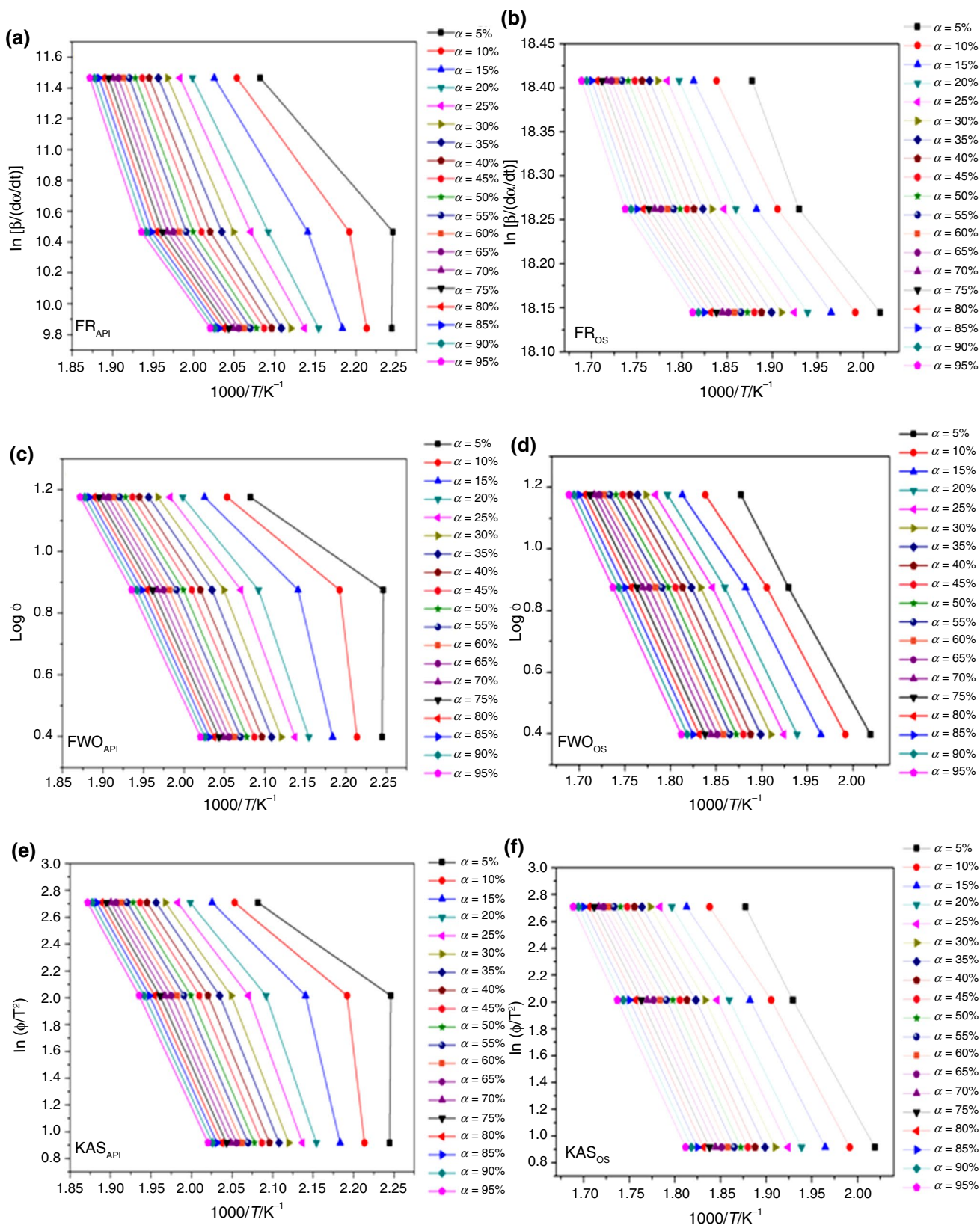
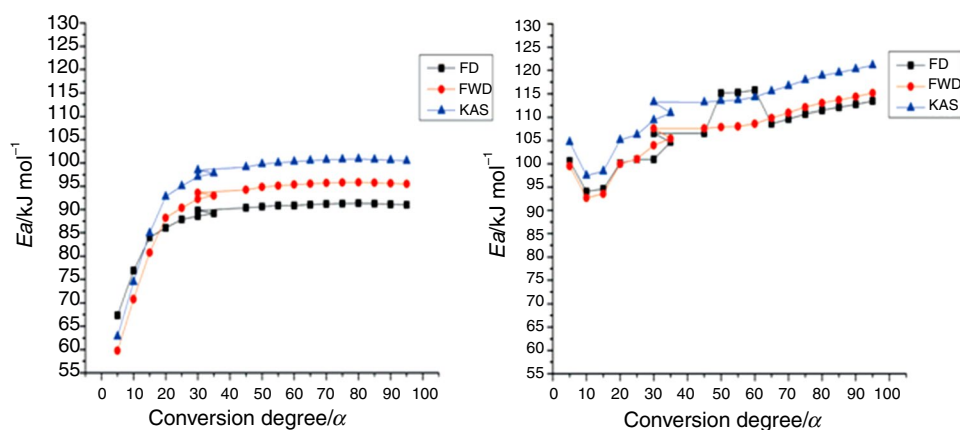


**Fig. 13** Graphic plots for the isoconversional methods: (a, b) Friedman, (c, d) Flynn–Wall–Ozawa and (e, f) Kissinger–Akahira–Sunose for EFZ and SD, respectively

**Fig. 14** Apparent  $E_a$  dependences on conversion according to FD, FWO, KAS method for EFZ and DS-PVPVA 64



conversion level. The presented accuracy for the conversion levels higher than 40% [28]. The lower linearization plot between 5 and 35% conversion level indicates changes of mechanisms of reaction of the degradation process.

In the Fig. 14, shown the values for apparent activation energy calculated by KAS, FD and FWO methods were similar throughout the degradation process. The EFZ presents lower  $E_a$  values that denotes lower stability. However, the higher  $E_a$  values for SD demonstrated increase of the stability the system [29].

In the Fig. 14, can also be observed that  $E_a$  values of EFZ showed increase in the decomposition process for the fractions from 5 to 35% (60 to 97  $\text{kJ mol}^{-1}$ ). For the conversion degree between 40 and 95%,  $E_a$  values had a discrete change from 98  $\text{kJ/mol}$  to 100  $\text{kJ/mol}$ . For SD PVPVA 64—EFZ 10%, show that chemical mechanism are similar, but the variance of  $E_a$  values variate from 100 to 120  $\text{kJ mol}^{-1}$ . Thus, it can be proposed that EFZ incorporated in SD, promotes increase of stability. The comparison of the activation energies obtained by all models

can be useful to estimate the probable thermodegradation kinetic mechanism of the EFZ and SD.

### Determination of degradation mechanism reaction

The  $E_a$  values obtained using the KAS method were used to determine the thermal degradation mechanisms proposed by Criado Method. This method uses reference theoretical curves proposed by functions described in Table 1. The Figs. 15 and 16 show the master curves for EFZ and SD.

It can be seen from Fig. 15 that for EFZ when the experimental value from 0.05 to 0.15 overlap the  $R_n$  curves these degradation mechanisms refer to a geometrical contraction. After this step degradation mechanism overlap the  $A_n$  curves until the end of process. When evaluating the thermal decomposition process of the SD PVPVA 64—EFZ 10% (Fig. 16), the same behavior was observed.

**Fig. 15** Master curves and experimental data obtained using the Criado method for EFZ

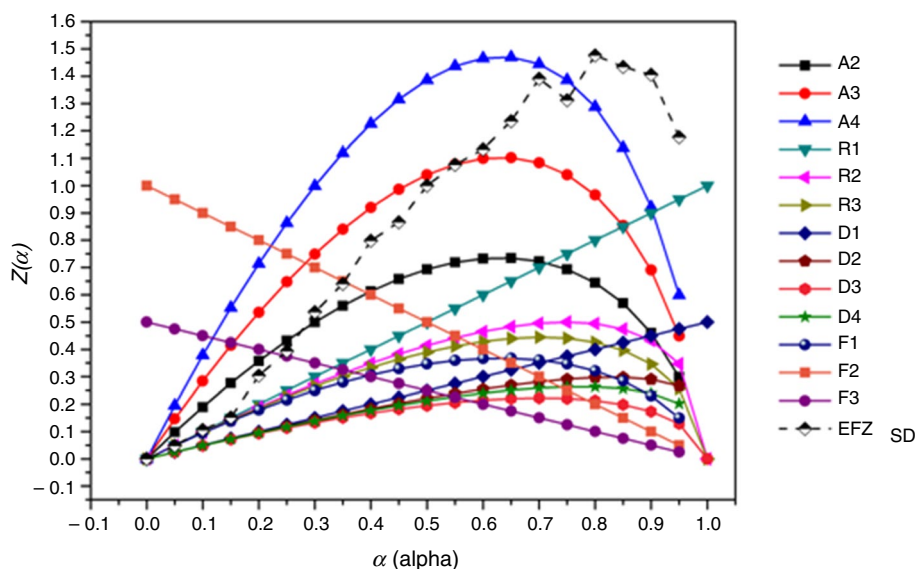
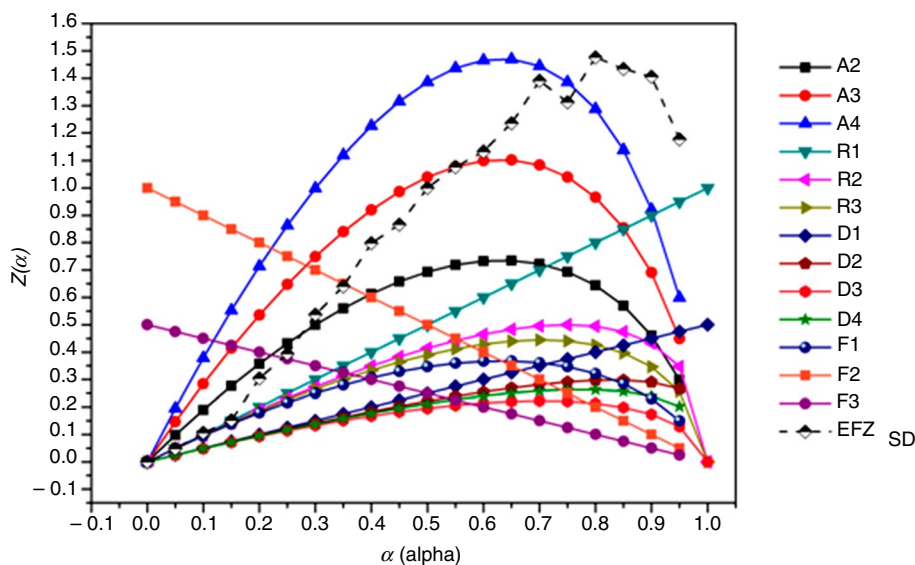


**Fig. 16** Master curves and experimental data obtained using the Criado method for SD PVPVA 64—EFZ 10%



Thus, the model-free analysis methods are easy to apply and are able to obtain kinetic parameters such activation energy as a function of reaction degree. As a main advantage, in the evaluation of the kinetic parameter, the use of isoconversion methods does not require knowledge of the reaction model.

## Conclusions

The study of the thermal behavior using thermoanalytical techniques allowed for the characterization of EFZ and its SD with PVPVA 64. It was shown that EFZ was converted to its amorphous state, and the polymer promoted a reduction in the molecular mobility of the system and, consequently, to the increase in the stability of the amorphous form of the drug.

Furthermore, it was found that the kinetics of thermal degradation of SD showed an order of 1 (one) for both methods, isothermal and non-isothermal. The values of the kinetic parameters, achieved by both models, are in agreement, and are located in a wide range ( $E_a = 101\text{--}132 \text{ kJ mol}^{-1}$ ). Thus, one may suggest an increase in EFZ thermal stability when it is dispersed in the polymer matrix, compared to the drug alone, guaranteeing a time of thermal stability in the formulation for approximately 7 months.

In addition, a good correlation between loss of mass and the Pyrolysis-GC-MS technique was observed. One can, also, suggest the formation of the same fragments obtained by hydrolysis, as well as, the promotion of the formation of other fragments which clarifies the technique with regard to the identification of thermal decomposition fragments.

Therefore, the thermal data provided important information on the evaluation of the stability of the formulation (SD), making it an important tool in quality control and pharmaceutical technology during product development.

**Acknowledgements** The authors would like to thank the Improving Coordination for Senior Staff (CAPES) and National Council of Scientific and Technological Development (CNPq) for financial support, Pharmaceutical Laboratory in the State of Pernambuco (LAFEPE) and the University of Toronto for the donation of raw materials and the Department of Pharmaceutical Sciences of the Federal University of Paraíba for performing the Pyrolysis-GC/MS analyses and DSC photo-visuals.

## References

1. Madhavi BB, Kusum B, Chatanya CHK, Madhu MN, Harsha VS, Banji D. Dissolution enhancement of efavirenz by solid dispersion and PEGylation techniques. *Int J Pharm Investig*. 2011. <https://doi.org/10.4103/2230-973X.76726>.
2. Sathigari S, Chada G, Lee YHP, Wright N, Parsons DL, Rangari VK, Fasina O, Babu RJ. Physicochemical characterization of efavirenz-cyclodextrin inclusion complexes. *AAPS PharmSciTech*. 2009. <https://doi.org/10.1208/s12249-008-9180-3>.
3. Sharma A, Jain CP. Solid dispersion: a promising technique to enhance solubility of poorly water soluble drug. *Int J Drug Deliv*. 2011;3:149–70.
4. Dinunzio JC, Brough C, Miller DA, Williams RO III, McGinity JW. Applications of KinetiSol® dispersing for the production of plasticizer free amorphous solid dispersions. *Eur J Pharm Sci*. 2010. <https://doi.org/10.1016/j.ejps.2010.03.002>.
5. Tiwari R, Tiwari G, Srivastava B, Rai AK. Solid dispersions: an overview to modify bioavailability of poorly water soluble drugs. *Int J PharmTech Res*. 2009;1:1338–49.

6. Oliveira MA, Yoshida MI, Gomes ECL. Análise térmica aplicada a fármacos e formulações farmacêuticas na indústria farmacêutica. *Quim Nova*. 2011;34:1224–30.
7. Baird JA, Taylor LS. Evaluation of amorphous solid dispersion properties using thermal analysis techniques. *Adv Drug Deliv Rev*. 2012. <https://doi.org/10.1016/j.addr.2011.07.009>.
8. Sovizi MR, Hosseini SG. Studies on the thermal behavior and decomposition kinetic of drugs cetirizine and simvastatin. *J Therm Anal Calorim*. 2013. <https://doi.org/10.1007/s10973-012-2651-5>.
9. Costa SPM, Silva KER, Medeiros GCR, Rolim LA, Oliveira JF, Lima MCA, Galdino SL, Pitta IR, Rolim-Neto PJ. Thermal behavior and compatibility analysis of the new chemical entity LPSF/FZ4. *Thermochim Acta*. 2013. <https://doi.org/10.1016/j.tca.2013.03.003>.
10. Fandaruff C, Araya-Sibaja AM, Pereira RN, Hoffmeister CRD, Rocha HVA, Silva MAS. Thermal behavior and decomposition kinetics of efavirenz under isothermal and non-isothermal conditions. *J Therm Anal Calorim*. 2014. <https://doi.org/10.1007/s10973-013-3306-x>.
11. Araújo AAS, Mercuri LP, Seixas SRS, Storpitis S, Matos JR. Determinação dos teores de umidade e cinzas de amostras comerciais de guaraná utilizando métodos convencionais e análise térmica. *Ver. Bras. Cienc. Farm*. 2006. <https://doi.org/10.1590/S1516-93322006000200013>.
12. Storpirtis S, Gonçalves JE, Chiann C, Gai MN. Ciências Farmacêuticas: Biofarmacotécnica. Rio de Janeiro: Guanabara Koogan; 2009.
13. Klancnik G, Medved J, Mrvar P. Differential thermal analysis (DTA) and differential scanning calorimetry (DSC) as a method of material investigation, *RMZ. Mater Geoenviron*. 2010;57:127–42.
14. Macêdo RO, Nascimento TG. Thermal characterization of lapa-chol by means of TG and DSC coupled to a photovisual system. *J Therm Anal Calorim*. 2001. <https://doi.org/10.1023/A:1011552613564>.
15. Silva RMF, Medeiros FPM, Nascimento TG, Macêdo RO, Rolim-Neto PJ. Thermal characterization of Indinavir sulfate using TG, DSC and DSC-photovisual. *J Therm Anal Calorim*. 2009. <https://doi.org/10.1007/s10973-008-8912-7>.
16. Viana OS, Araujo AAS, Simões RA, Soares JL, Matos CRS, Grangeiro SC Jr, Lima M, Rolim-Neto PJ. Kinetic analysis of the thermal e composition of efavirenz and compatibility studies with selected excipients. *Lat Am J Pharm*. 2008;27:211–6.
17. Brown ME. Introduction to the thermal analysis. Techniques and applications. 2nd ed. Dordrecht: Kluwer Academic Publishers; 2001.
18. Jankovic B, Mentus S, Jankovic M. A kinetic study of the thermal decomposition process of potassium metabisulfite: estimation of distributed reactivity model. *J Phys Chem Solids*. 2008;69:1923–33.
19. Moura EA, Correia LP, Pinto MF, Procópio JVV, Souza FS, Macêdo RO. Thermal characterization of the solid state and raw material fluconazole by thermal analysis and pyrolysis coupled to GC/MS. *J Therm Anal Calorim*. 2010. <https://doi.org/10.1007/s10973-009-0473-x>.
20. Oliveira AH, Moura EA, Pinto MF, Procópio JVV, Souza VG, Souza FS, Macêdo RO. Thermal characterization of raw material pentoxifylline using thermoanalytical techniques and Pyr-GC/MS. *J Therm Anal Calorim*. 2011. <https://doi.org/10.1007/s10973-011-1839-4>.
21. Boer TM, Procópio JVV, Nascimento TG, Macêdo RO. Correlation of thermal analysis and pyrolysis coupled to GC–MS in the characterization of tacrolimus. *J Pharm Biomed Anal*. 2013. <https://doi.org/10.1016/j.jpba.2012.01.040>.
22. Kolter K, Karl M, Gryczke A. Hot-melt extrusion with BASF pharma polymers: extrusion compendium 2nd revised and enlarged edition. BASF SE Pharma Ingredients & Services. 2012. [http://www.pharmaingredients.basf.com/Documents/ENP/Brochure/EN/03\\_120803%20Hot%20Melt%20Extrusion%20with%20BASF%20Pharma%20Polymers.pdf](http://www.pharmaingredients.basf.com/Documents/ENP/Brochure/EN/03_120803%20Hot%20Melt%20Extrusion%20with%20BASF%20Pharma%20Polymers.pdf). Accessed 25 Feb 2015.
23. Maurin MB, Roew SM, Blom K, Pierce ME. Kinetics and mechanism of hydrolysis of efavirenz. *Pharm Res*. 2002. <https://doi.org/10.1023/A:1015160132290>.
24. Beyler CL, Hirschler MM. Thermal decomposition of polymers. In: DiNenno PJ, editor. SFPE handbook of fire protection engineering. Bethesda, MA: Springer; 2002. p. 110–31.
25. Macêdo RO, Nascimento TG. Quality control of thiaabendazole pre-formulation and tablets by TG and DSC coupled to the photovisual system. *Thermochim Acta*. 2002. [https://doi.org/10.1016/S0040-6031\(02\)00088-6](https://doi.org/10.1016/S0040-6031(02)00088-6).
26. Teja SB, Patil SP, Shete G, Patel S, Bansal AK. Drug-excipient behavior in polymeric amorphous solid dispersions. *J Excip Food Chem*. 2013;4:70–94.
27. Tita B, Jurca T, Tita D. Thermal stability of pentoxifylline: active substance and tablets. Part 1. Kinetic study of the active substance under non-isothermal conditions. *J Therm Anal Calorim*. 2013. <https://doi.org/10.1007/s10973-013-3118-z>.
28. Mohamed MA, Attia AK. Thermal behavior and decomposition kinetics of cinnarizine under isothermal and non-isothermal conditions. *J Therm Anal Calorim*. 2016. <https://doi.org/10.1007/s10973-016-5551-2>.
29. Bianchi O. Avaliação da Degradação Não-Isotérmica de Madeira Através de Termogravimetria-TGA. *Polímeros*. 2010.

**Publisher's Note** Springer Nature remains neutral with regard to jurisdictional claims in published maps and institutional affiliations.